Electrical Power and Energy Systems 116 (2020) 105546

Contents lists available at ScienceDirect

Electrical Power and Energy Systems

journal homepage: www.elsevier.com/locate/ijepes

Grounding grids in electro-magnetic transient simulations with frequency-dependent equivalent circuit

Manunza Alessandro*

Electrical Engineer, M2EC, Italy

ARTICLE INFO

Keywords:
Grounding grids
Fast transients
ATP-EMTP
Frequency-dependent equivalent circuit

ABSTRACT

The frequency behaviour of a grounding grid cannot be neglected in insulation coordination studies. This paper proposes a new approach, which consists of calculating the frequency behaviour of a grounding grid by means of a software which implements the electromagnetic theory, building a two-port component, whose internal admittances are defined as rational functions in the Laplace domain, and finally using this two-port component for time-domain fast transient simulations.

1. Introduction

The behaviour of a grounding grid at power frequencies is well-known, while the behaviour during a fast transient is much more complicated because it requires the knowledge of the physics of a grounding grid in a wide frequency range. Probably for this reason, grounding grids of Overhead Line (OHL) towers are usually simulated by resistors, whose resistances are measured or calculated at power frequency. However, this simple model is not adequate to simulate the physical phenomena during high frequency transients, like those related to lightning. Furthermore, the grounding grids of substations are usually neglected and their components are connected to the ideal ground node, which is the zero-potential node, or they are represented by a resistor, whose resistance is calculated at power frequency. This could be a vague simplification because, from the physical point of view, each grounding grid conductor is coupled with any other conductor by resistive, inductive and capacitive phenomena as well as with all the soil. This means that part of the voltage wave injected in the grounding grid can travel along these buried conductors, while another part is dispersed into the ground. Consequently, different conductors of the grounding grid have different potentials and their impedances are frequency-dependent.

In order to simulate grounding grids, technical literature reports several studies that can be grouped in three main categories:

- The Network Approach, based circuit theory methods, including distributed parameters typically used for transmission line modelling.
- The Electromagnetic Approach is based on the electromagnetic theory and with the least neglects possible.
- Hybrid Approach, which applies the electromagnetic theory to obtain an equivalent circuit.

The transmission line approach is a suitable for the considered frequency range and it allows the simulation of even the non-linear phenomenon of soil ionization, but it could be difficult to apply to large grounding grids [4,7,11,13,14].

The electromagnetic approach allows the construction of a complete model, but is difficult to interface with software programs for the simulation of power systems subject to fast transients.

The hybrid approach can implement most of the advantages of the electromagnetic approach but permits building a model that can be integrated inside software for transient simulations [3,5,9,12,15,16,17].

After neglecting the breakdown phenomena of the soil ionisation and the mutual coupling between underground and above-ground structures, this paper proposes a new hybrid approach, which consists of three steps:

1. Use of software, named XGSLab [18], to calculate the frequency behaviour of a grounding grid;
2. Building a two-port component, whose internal admittances are defined as rational functions in the Laplace domain;
3. Finally, the two-port component is used in software, named ATP-EMTP [1], for time-domain fast transient simulations.

The proposed method is similar to the one described in [17]. The main difference lies in how the grounding grid is modelled in ATP-

* Address: Manunza Alessandro, Via Copernico n°5, 09060 Settimo San Pietro (CA), Italy.
E-mail address: m2ec@manunza.com.

https://doi.org/10.1016/j.ijepes.2019.105546
Received 12 April 2019; Received in revised form 11 July 2019; Accepted 10 September 2019

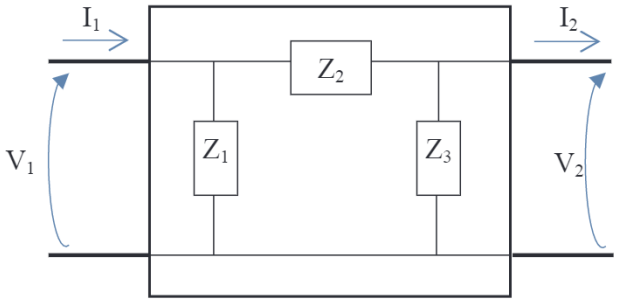

Fig. 1. Equivalent circuit.

EMTP: the authors of [17] represented the grounding grid by means of two branches in parallel. Each branch is composed by a rational function in the Laplace domain and a voltage source controlled by an algorithm written in language MODELS. This language is interpreted during the simulation and consequently is time consuming. The grounding grid model proposed in this paper is composed by a simple passive network of components, which are directly implemented inside ATP-EMTP. The proposed approach is more straightforward and less time consuming and can be applied to any kind of soil model and any shape of grounding grid.

2. High frequency model

In an HV substation, usually an incoming voltage surge (V_A) is partially diverted to ground by surge arresters. While part of the voltage wave (V_B) travels through the grounding grid, the remainder (V_C) continues to travel through phase conductors to the most delicate circuit component: the transformer, which is usually characterised by the highest surge impedance. The wave V_B enters the grounding grid where the surge arrester is grounded and travels through the grounding electrode where it is also partially dispersed into the ground. This dispersion causes a rise of the potential of the soil and of the electrode conductors. The higher the frequency is, the greater the amount of the current dispersed near the entry point. Nevertheless, the point of the grounding grid where the transformer is grounded is affected by a potential rise due to the wave travelling in the grounding grid. Definitely a grounding grid, affected by a voltage wave, cannot be considered as equipotential, much less its potential is zero.

Building a high frequency model of each element of a grounding grid, including all the possible mutual coupling, is extremely onerous and, in our opinion, not necessary for practical applications. It is

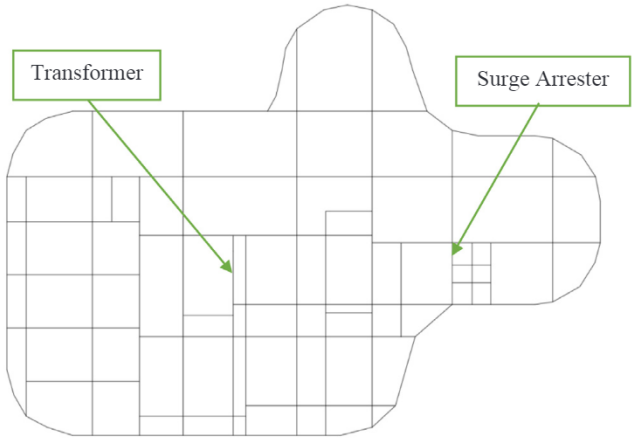

Fig. 3. Substation grounding grid.

deemed sufficient to model it as a two-port component: port 1 corresponds to the point of connection of the surge arrester, while port 2 is the point of connection of the transformer. The chosen internal model for this two-port component is a PI circuit, composed by $Z_1(\omega)$, $Z_2(\omega)$ and $Z_3(\omega)$, shown in Fig. 1. $Z_1(\omega)$ and $Z_3(\omega)$ allow the simulation of the current dispersed into the ground in correspondence of the surge arrester and the transformer, while $Z_2(\omega)$ allows the modelling of the wave propagation between these two points.

In order to determine $Z_1(\omega)$, $Z_2(\omega)$ and $Z_3(\omega)$, it is necessary to undertake two (calculated or measured) short-circuit tests at different frequencies.

Test (a): short circuit at port 2. Given $V_{2a} = 0$, it is possible to write $V_{1a} = Z_2\ I_{2a}$ and $V_{1a} = Z_1\ (I_{1a} - I_{2a})$. Consequently, the following equations can be written $\mathbf{Z_2 = V_{1a}/I_{2a}}$ and $\mathbf{Z_1 = V_{1a}/(I_{1a} - I_{2a})}$.

Test (b): short circuit at port 1. Given $V_{1b} = 0$, it is possible to write $V_{2b} = -Z_2\ I_{1b}$ and $V_{2b} = Z_3\ (-I_{2b} + I_{1b})$. Consequently, the following equations can be written $\mathbf{Z_2 = -V_{2b}/I_{1b}}$ and $\mathbf{Z_3 = V_{2b}/(I_{1b} - I_{2b})}$.

In this paper four different frequency values per decade have been considered up to 2 MHz, starting from 20 Hz. The calculation results consist of a matrix of impedance amplitudes and phase angles for each impedance. These impedance matrices can be converted into admittance matrices and then into rational transfer functions by applying the ARMA algorithm [14]. The three rational transfer functions can be associated to three ATP-EMTP components named "Kizilcay F-dependent Branch" [8]. These components $Y_1(\omega)$, $Y_2(\omega)$ and $Y_3(\omega)$ are to be properly connected to obtain the desired PI equivalent.

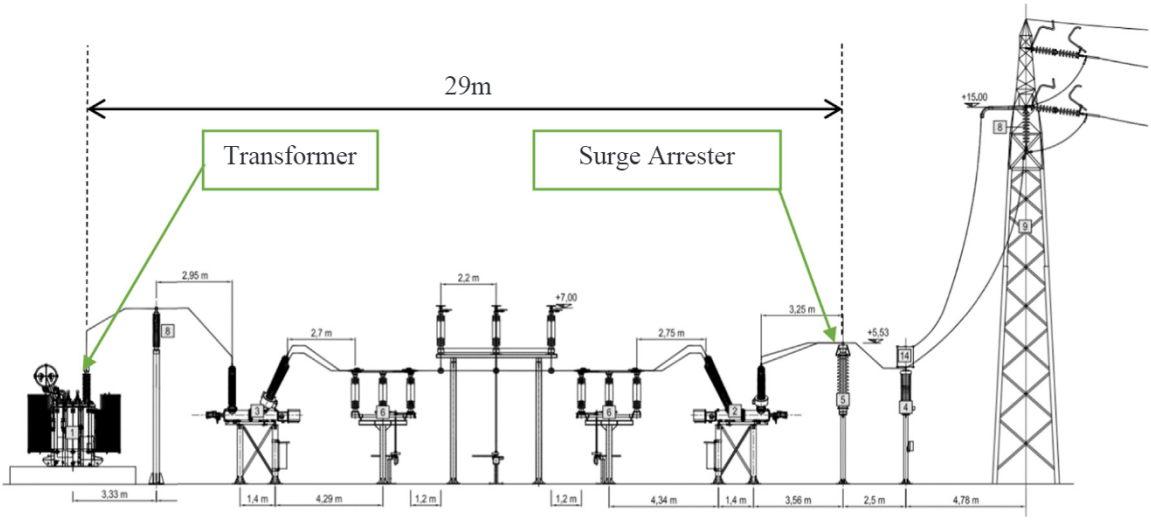

Fig. 2. Substation side view.

Table 1
Results of test (a): short circuit at transformer location.

f (Hz)	|V1| (V)	∠V1 (°)	|I1| (A)	∠I1 (°)	|I2| (A)	∠I2 (°)	|Z2| (Ω)	∠Z2 (°)	|Z1| (Ω)	∠Z1 (°)
20	3.18E−03	50.031	1	0	0.999	−0.067	3.18E−03	50.098	2.06E+00	0.614
50	6.41E−03	71.123	1	0	0.999	−0.167	6.41E−03	71.29	2.08E+ 00	0.152
70	8.74E−03	76.075	1	0	0.999	−0.234	8.75E−03	76.309	2.08E+ 00	−0.043
100	1.23E−02	79.883	1	0	0.999	−0.334	1.23E−02	80.217	2.08E+00	−0.211
200	2.43E−02	84.188	1	0	0.999	−0.667	2.43E−02	84.855	2.08E+00	−0.566
500	6.02E−02	85.922	1	0	0.998	−1.663	6.03E−02	87.585	2.07E+00	0.699
700	8.39E−02	85.764	1	0	0.998	−2.323	8.41E−02	88.087	2.07E+00	−0.248
1000	1.19E−01	85.173	1	0	0.996	−3.307	1.20E−01	88.48	2.07E+00	0.798
2000	2.34E−01	82.651	1	0	0.99	−6.536	2.37E−01	89.187	2.06E+00	0.948
5000	5.55E−01	75.213	1	0	0.955	−15.744	5.81E−01	90.957	2.04E+00	2.537
7000	7.43E−01	70.809	1	0	0.921	−21.393	8.07E−01	92.202	2.04E+00	3.788
10,000	9.87E−01	65.159	1	0	0.861	−29.002	1.15E+00	94.161	2.04E+00	5.768
2.00E+04	1.53E+00	53.43	1	0	0.657	−47.227	2.33E+00	100.657	2.08E+00	12.381
5.00E+04	2.28E+00	45.839	1	0	0.336	−68.198	6.78E+00	114.037	2.45E+00	26.220
7.00E+04	2.64E+00	45.89	1	0	0.25	−73.234	1.06E+01	119.124	2.75E+00	31.424
1.00E+05	3.14E+00	46.546	1	0	0.18	−77.235	1.74E+01	123.781	3.21E+00	36.185
2.00E+05	4.53E+00	46.95	1	0	0.093	−81.734	4.87E+01	128.684	4.57E+00	41.621
5.00E+05	7.15E+00	45.617	1	0	0.044	−84.816	1.63E+02	130.433	7.17E+00	43.098
7.00E+05	8.36E+00	45.81	1	0	0.035	−89.723	2.39E+02	135.533	8.36E+00	43.805
1.00E+06	9.89E+00	46.719	1	0	0.028	−99.341	3.53E+02	146.06	9.84E+00	45.144
2.00E+06	1.43E+01	49.774	1	0	0.018	−136.26	7.93E+02	186.031	1.41E+01	49.070

Table 2
Results of test (b): short circuit at surge arrester location.

f (Hz)	|V2| (V)	∠V2 (°)	|I1| (A)	∠I1 (°)	|I2| (A)	∠I2 (°)	|Z2| (Ω)	∠Z2 (°)	|Z3| (Ω)	∠Z3 (°)
20	3.18E−03	50.008	0.999	−0.089	1	0	3.18E−03	50.097	1.72E+00	−7.162
50	6.41E−03	71.068	0.999	−0.222	1	0	6.41E−03	71.29	1.60E+00	−4.342
70	8.74E−03	75.999	0.999	−0.31	1	0	8.75E−03	76.309	1.59E+00	−3.369
100	1.23E−02	79.775	0.999	−0.442	1	0	1.23E−02	80.217	1.58E+00	−2.614
200	2.43E−02	83.973	0.998	−0.882	1	0	2.43E−02	84.855	1.57E+00	1.824
500	6.01E−02	85.398	0.997	−2.188	1	0	6.03E−02	87.586	1.57E+00	0.990
700	8.38E−02	85.04	0.996	−3.048	1	0	8.41E−02	88.088	1.57E+00	0.872
1000	1.19E−01	84.162	0.993	−4.321	1	0	1.20E−01	88.483	1.57E+00	1.641
2000	2.32E−01	80.794	0.978	−8.398	1	0	2.37E−01	89.192	1.58E+00	3.607
5000	5.25E−01	72.113	0.904	−18.857	1	0	5.80E−01	90.97	1.61E+00	8.431
7000	6.82E−01	67.949	0.845	−24.27	1	0	8.07E−01	92.219	1.64E+00	11.425
10,000	8.72E−01	63.777	0.76	−30.406	1	0	1.15E+00	94.183	1.69E+00	15.627
2.00E+04	1.32E+00	59.384	0.566	−41.313	1	0	2.33E+00	100.697	1.92E+00	26.361
5.00E+04	2.34E+00	60.732	0.345	−53.377	1	0	6.78E+00	114.109	2.78E+00	41.511
7.00E+04	2.96E+00	61.195	0.28	−58.016	1	0	1.06E+01	119.211	3.35E+00	45.614
1.00E+05	3.82E+00	60.961	0.219	−62.924	1	0	1.75E+01	123.885	4.15E+00	48.740
2.00E+05	6.21E+00	58.477	0.128	−70.351	1	0	4.85E+01	128.828	6.44E+00	51.297
5.00E+05	1.11E+01	52.616	0.067	−78.033	1	0	1.65E+02	130.649	1.12E+01	48.813
7.00E+05	1.34E+01	50.304	0.056	−85.471	1	0	2.39E+02	135.775	1.34E+01	47.095
1.00E+06	1.62E+01	47.984	0.045	−98.331	1	0	3.59E+02	146.315	1.60E+01	45.451
2.00E+06	2.27E+01	44.44	0.029	−141.788	1	0	7.82E+02	186.228	2.22E+01	43.435

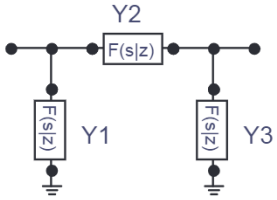

Fig. 4. Equivalent circuit as represented in ATPDraw.

The proposed two-port component does not take into account the breakdown phenomenon of the soil ionisation, which occurs for high currents and for high values of the electric field in the soil as stated in [4], and the mutual coupling between underground and above-ground structures.

3. Case of study

The method described in Section 2 has been applied to an existing 150 kV substation in order to verify the feasibility of the proposed method, the correctness of the equivalent model and the consequence on insulation coordination studies.

Fig. 2 shows the side view of the substation, where the positions of the three-phase surge arrester and of the transformer are indicated. The distance between them is about 29 m.

Fig. 3 shows the grounding grid and where the surge arrester and the transformer are connected.

3.1. Modelling of the electrode in XGSLab

The grounding grid is modelled in XGSLab [18] and the electrode is constructed of round copper conductors with an external diameter of 12 mm. The grid is buried at a depth of 0.6 m in a uniform soil whose resistivity $\rho = 100\,\Omega$m and relative permittivity $\varepsilon = 6$, both of which are assumed to be frequency independent. For the short circuit tests, the short circuit is modelled as a transversal impedance of $10^{-4}\,\Omega$ connected to the grounding grid and to the remote earth (potential zero of XGSLab [18]), while a current of 1A with a phase angle of 0° is injected.

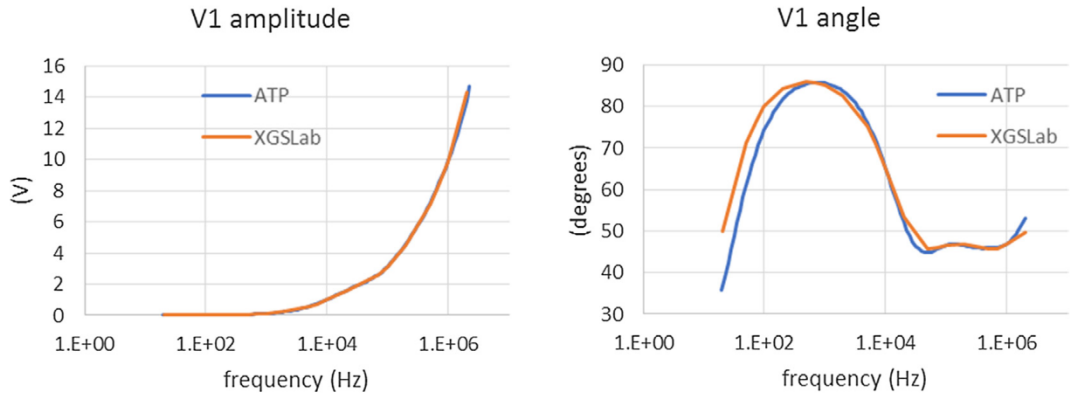

Fig. 5. Comparison of results for a short circuit at transformer location.

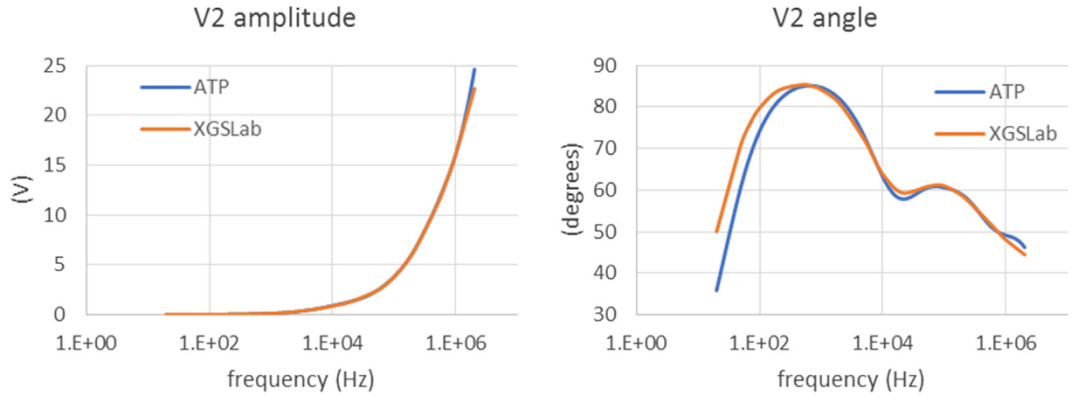

Fig. 6. Comparison of results for a short circuit at surge arrester location.

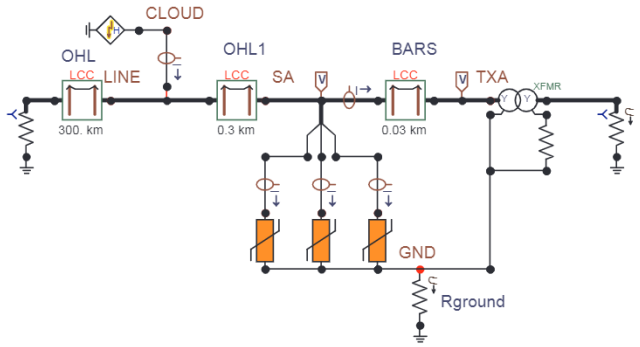

Fig. 7. Test circuit with the grounding grid represented by a resistor.

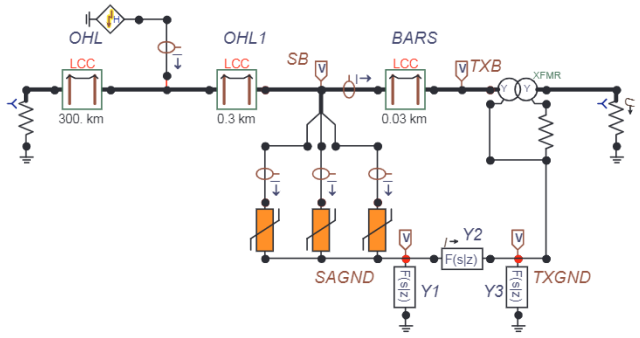

Fig. 8. Circuit with the frequency-dependent model of the grounding grid.

Results of test (a): short circuit at transformer location (see Table 1)
Results of test (b): short circuit at surge arrester location (see Table 2)

3.2. Rational transfer functions

The numerical values of $Z_1(\omega)$, $Z_2(\omega)$ and $Z_3(\omega)$ are converted into numerical admittances $Y_1(\omega)$, $Y_2(\omega)$ and $Y_3(\omega)$. Applying the ARMA algorithm [2], $Y_1(\omega)$, $Y_2(\omega)$ and $Y_3(\omega)$ are converted into following rational functions in the Laplace domain:

$$Y_1 = \frac{3.072 \times 10^{-22}s^3 + 9.016 \times 10^{-14}s^2 + 5.262 \times 10^{-7}s + 0.49}{6.708 \times 10^{-20}s^3 + 1.140 \times 10^{-12}s^2 + 2.775 \times 10^{-6}s + 1.0} \quad (1)$$

$$Y_2 = \frac{3.676 \times 10^{-19}s^3 - 1.498 \times 10^{-11}s^2 + 1.794 \times 10^{-4}s + 316}{6.773 \times 10^{-16}s^3 + 1.205 \times 10^{-8}s^2 + 5.955 \times 10^{-3}s + 1.0} \quad (2)$$

$$Y_3 = \frac{2.210 \times 10^{-20}s^3 + 6.523 \times 10^{-13}s^2 + 1.792 \times 10^{-6}s + 0.626}{1.105 \times 10^{-18}s^3 + 8.754 \times 10^{-12}s^2 + 7.173 \times 10^{-6}s + 1.0} \quad (3)$$

These rational functions are directly implemented in EMTP-ATP by means of the component named "KIZILCAY F-DEPENDENT branch" [8]. Fig. 4 shows the circuit equivalent to the grounding grid as represented in the EMTP-ATP graphical environment named ATPDraw.

To validate the equivalent circuit, the short circuit tests are repeated with EMTP-ATP and the results compared.

The results concerning test (a), short circuit at transformer location, are shown in Fig. 5 while Fig. 6 shows the results of test (b), short circuit at surge arrester location.

Figs. 5 and 6 demonstrate that the equivalent circuit built in EMTP-ATP has a frequency behaviour very close to the one calculated by XGSLab. This confirms that it is possible to reproduce the frequency behaviour of a grounding grid inside an environment for the time-domain simulation of electromagnetic transients (EMTP-ATP).

4. Impact of grounding grids in EMTs

In order to evaluate the impact of a grounding grid on the results of

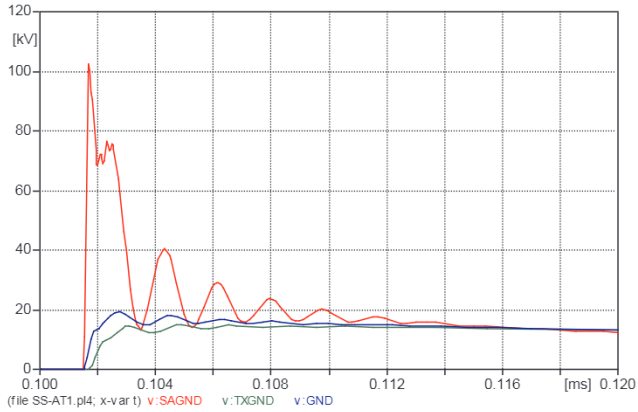

Fig. 9. GPR at GND (Blue), SAGND (red) and TXGND (green). (For interpretation of the references to colour in this figure legend, the reader is referred to the web version of this article.)

an insulation coordination study, a simple test circuit has been considered for the substation shown in Fig. 2. This circuit consists of a 300 km, 150 kV Overhead Line (OHL), 150 kV surge arresters, 30 m busbars and 150/15 kV, 40 MVA transformer. A 20 kA lightning stroke is applied on phase A of the OHL at a distance of 300 m from the substation.

4.1. Modelling of the power system

The Overhead Line (OHL) is represented by means of the J-Marti frequency dependent model, considering the conductor cross section and material, the geometry of a typical 150 kV pole.

The 30 m busbars are modelled by KCLee or Clark model (Bergeron model) at a frequency of 500 kHz.

The 150/15 kV, 40 MVA transformer is modelled by means of the Hybrid Transformer component, which includes the capacitive couplings among windings.

The lightning is modelled by the Heidler function with a peak value of 20 kA and the waveform of 1.2/50 μs.

The frequency-dependent model of the surge arresters (SA) is based on papers [6] and [10], which allow the parameters of the model to be determined from the data reported in the datasheets [19] for the SA model ABB EXLIM Q144-EH170.

Taking into account the minimum travelling time of the voltage waves in cables and lines, the simulation time step is chosen equal to 10^{-8} s.

Fig. 7 shows the test circuit where the grounding grid is represented by a 0.89 Ω resistor, whose resistance is calculated at 50 Hz by means of XGSLab. While Fig. 8 shows the test circuit where the grounding grid is represented by the calculated frequency-dependent model.

4.2. Simulation results

The first important results are shown in Fig. 9 where the Ground Potential Rise (GPR) at the grounding point of the surge arresters (node SAGND) and of the transformer (node TXGND), which are calculated considering the frequency-dependent model of the grounding grid, are compared with the GPR at node GND of Fig. 7, which is calculated considering a resistor to model the grounding grid.

The potential at node SAGND has a peak value of 113 kV and some oscillations superposed on the decreasing exponential tail. The ground potential at the transformer grounding point (TXGND) starts raising after 0.35 μs compared to SAGND, due to the travelling time of the voltage wave throughout the grounding grid, and has a much lower peak (15 kV) but a similar long tail. Most of the ground potential rise is around the surge arrester, but the ground potential rise at the transformer is certainly not negligible. When the grounding grid is modelled with a resistor, the GPR starts raising immediately but the peak value is limited to 20 kV.

Fig. 10 demonstrates that the current drawn by the Phase A surge arrester is almost the same in both test circuits as well as the potential difference at its terminals. The presence of the proposed grounding grid model does not affect the behaviour of the surge arrester.

Fig. 11 clearly shows the impact of the grounding grid model on the test circuit: if the grounding grid is represented by a resistor, then the peak value of the voltage at the transformer terminals is about 784 kV, while the voltage peak is about 915 kV when the grounding grid is simulated by the proposed model. Taking into account the standard lightning impulse withstand voltage of the transformer and of the other electrical components, the consequences on the substation design can be risky. This result, besides confirming the well-known criteria of installing surge arresters close to the components to be protected, demonstrates the importance of including proper models of grounding grids in the simulations of fast transients.

5. Conclusions

Grounding grids for fast transient simulations can be modelled by applying the Network Approach, which is based upon circuit theory methods, or the Electromagnetic Approach is based on the electromagnetic theory. This paper proposes a new hybrid approach, which consists of calculating the frequency behaviour of a grounding grid, building a two-port component, whose internal admittances are defined as rational functions in the Laplace domain, and finally using this two-

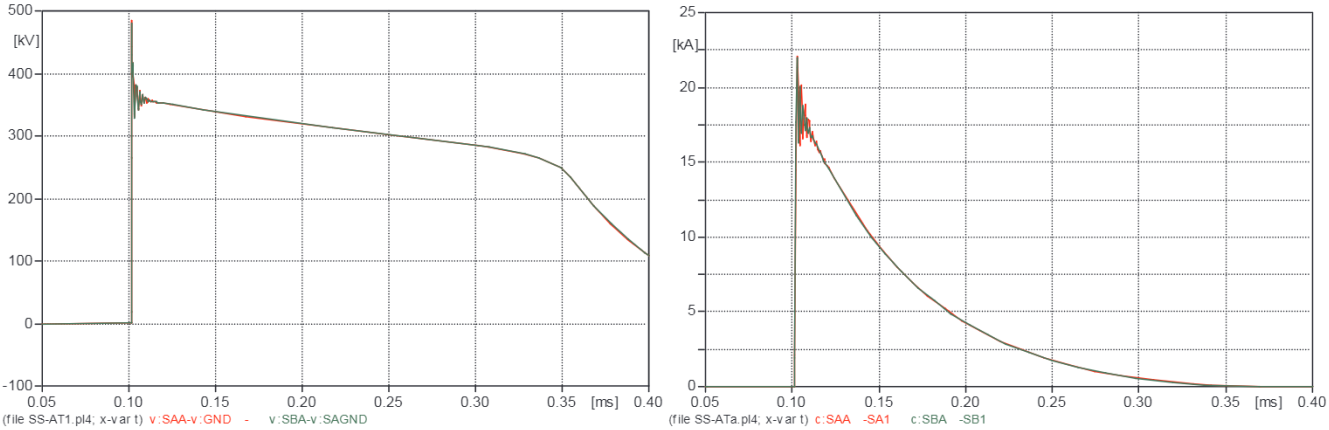

Fig. 10. Currents and voltages of Phase A surge arrester if the grounding grid is represented by the frequency-dependent model (green) and by a resistor (red). (For interpretation of the references to colour in this figure legend, the reader is referred to the web version of this article.)

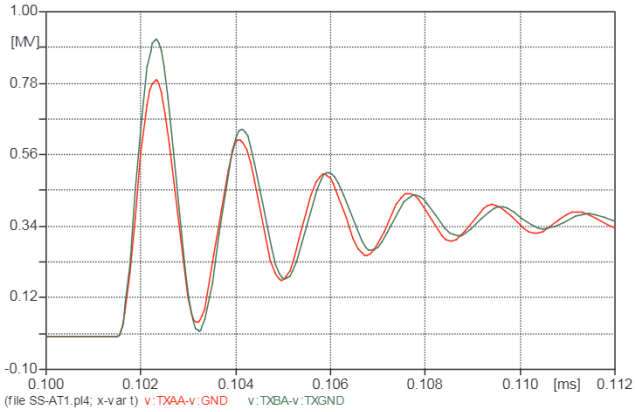

Fig. 11. Potential difference between the transformer terminal and its grounding point if the grounding grid is represented by the high frequency model (green) and by a resistor (red). (For interpretation of the references to colour in this figure legend, the reader is referred to the web version of this article.)

port component for time-domain fast transient simulations.

The proposed method is simple to apply to any kind of grounding grid and any kind of soil. The grounding grid is converted into an equivalent PI circuit composed only by three passive, frequency-dependent components. This allows to save computational time because the passive components are directly implemented inside the software for time-domain fast transient simulations. On the other hand, rational functions are not able to represent non-linear phenomena, like soil ionisation. But soil ionisation is important only for small electrodes and very large currents.

The application of the proposed method to a real case has demonstrated that:

- The two-port component has a frequency behaviour very close to the one calculated for the grounding grid.
- The two-port component allows the simulation of the propagation of voltage waves in the grounding grid and the differing ground potential rises in different locations.
- Grounding grids are absolutely not negligible in fast transient simulations and above all in insulation coordination studies.

Declaration of Competing Interest

The authors declared that there is no conflict of interest.

Appendix A. Supplementary material

Supplementary data to this article can be found online at https://doi.org/10.1016/j.ijepes.2019.105546.

References

[1] Canadian/American EMTP User Group. Alternative transients program (ATP) – rule book; 1992–2000.
[2] Noda T, Nagaoka N. Development of ARMA models for a transient calculation using linearized least-squares method. TransIEE Jpn 1994;114-B(4):396–402.
[3] Mentre FE, Grcev L. EMTP-based model for grounding system analysis. IEEE Trans Power Del 1994;9(4).
[4] Heimbach M, Grcev LD. Grounding system analysis in transients programs applying electromagnetic field approach. IEEE Trans Power Del 1997;12(1).
[5] Grcev LD, Heimbach M. Frequency dependent and transient characteristics of substation grounding systems. IEEE Trans Power Del 1997;12(1).
[6] Pinceti P, Giannettoni M. A simplified model for zinc oxide surge arresters. IEEE Trans. PWD 1999;14(2):393–7.
[7] Liu Y, Zitnik M, Thottappillil R. An improved transmission-line model of grounding system. IEEE Trans Electromagn Compat 2001;43(3).
[8] Kizilcay. Generation of network equivalent using ARMAFIT program and kizilcay F-dependent branch. EEUG News 2001;7(3).
[9] Grcev L, Arnautovski-Toseva V. Grounding systems modeling for high frequencies and transients: some fundamental considerations. IEEE bologna power tech conference proceedings. 2003.
[10] Giannettoni, Magro, Pinceti. Validation of ZnO surge arresters model for overvoltage studies. IEEE Trans PWD 2004;19:1692–5.
[11] Liu Y, Theethayi N, Thottappillil R. An engineering model for transient analysis of grounding system under lightning strikes: non uniform transmission-line approach. IEEE Trans Power Del 2005;20(2).
[12] Grcev L, Popov M. On high-frequency circuit equivalents of a vertical ground rod. IEEE Trans Power Del 2005;20(2):1598–603.
[13] Zeng Rong, Kang Peng, He Jinliang, Zhang Bo, Chen Shuiming, Zou Jun. Lightning transient performance analysis of substation based on complete transmission line model of power network and grounding systems. IEEE Trans Magn 2006;42(4).
[14] Zeng R, Gong X, He J, Zhang B, et al. Lightning impulse performances of grounding grids for substations considering soil ionization. IEEE Trans Power Del 2008;23(2).
[15] Sarajcev P, Vujevic S, Lovric D. Interfacing harmonic electromagnetic models of grounding systems with the EMTP-ATP software package. Renew Energy 2014;68:163–70.
[16] Ahmadi N, Mashayekhi V, et al. Frequency-dependent modeling of grounding system in EMTP for lightning transient studies of grid-connected PV systems. International conference on renewable energy research and applications (ICRERA). 2015.
[17] Popov M, Grcev L, Høidalen HKr, Gustavsen B, Terzija V. Investigation of the overvoltage and fast transient phenomena on transformer terminals by taking into account the grounding effects. IEEE Trans Ind Appl 2015;51(6):5218–27.
[18] Sint Ingegneria, XGSLab user's guide. https://www.xgslab.com/.
[19] ABB, Surge arrester buyers guide – EXLIM Q144-EH170.